J. Fluid Mech. (2000), *vol.* 410, *pp.* 263–283. Printed in the United Kingdom

Self-similar intermediate structures in turbulent boundary layers at large Reynolds numbers

By G. I. BARENBLATT[1], A. J. CHORIN[1] AND V. M. PROSTOKISHIN[2]

[1] Department of Mathematics and Lawrence Berkeley National Laboratory, University of California, Berkeley, CA 94720, USA

[2] P. P. Shirshov Institute of Oceanology, Russian Academy of Sciences, 36 Nakhimov Prospect, Moscow 117218, Russia

(Received 10 May 1999 and in revised form 13 December 1999)

Processing the data from a large variety of zero-pressure-gradient boundary layer flows shows that the Reynolds-number-dependent scaling law, which the present authors obtained earlier for pipes, gives an accurate description of the velocity distribution in a self-similar intermediate region adjacent to the viscous sublayer next to the wall. The appropriate length scale that enters the definition of the boundary layer Reynolds number is found for all the flows under investigation.

Another intermediate self-similar region between the free stream and the first intermediate region is found under conditions of weak free-stream turbulence. The effects of turbulence in the free stream and of wall roughness are assessed, and conclusions are drawn.

1. Introduction

Asymptotic laws for wall-bounded turbulent shear flows at large Reynolds numbers are considered. Classical examples of such flows are those in pipes, channels, and boundary layers. This class of flows is of major fundamental and practical importance. All these flows share as dimensional governing parameters the shear stress at the wall τ and the fluid's properties: its density ρ and dynamic viscosity μ. From these parameters two important quantities can be formed: the *dynamic* or *friction* velocity $u_* = (\tau/\rho)^{1/2}$ and the length scale $\delta = \nu/u_*$, where $\nu = \mu/\rho$ is the fluid's kinematic viscosity. The length scale δ is tiny at large Reynolds numbers, and in the layer where the dimensionless distance from the wall y/δ is less than, say, 70 (viscous sublayer) the viscous stress is comparable with the Reynolds stress created by vortices. Outside this viscous sublayer, at $y/\delta > 70$, the contribution of the viscous stress is small. We emphasize that 'small' is not always synonymous with 'negligible', and indeed we will see that here is a case where it is not.

In 1930, Th. von Kármán proposed in explicit form the hypothesis that outside the viscous sublayer the contribution of viscosity can be neglected. On the basis of this assumption he derived the *universal* (i.e. Reynolds-number independent) *logarithmic law* for the distribution of the mean velocity u over the cross-section:

$$\phi = \frac{u}{u_*} = \frac{1}{\kappa}\ln\eta + C, \quad \eta = \frac{u_* y}{\nu}, \tag{1}$$

where y is the distance from the wall; the constants κ (the von Kármán constant) and C should be identical for all turbulent wall-bounded shear flows at high Reynolds numbers, and the law (1) should be valid in intermediate regions between, on one hand, the viscous sublayer and, on the other, the external parts of the flows, e.g. the vicinity of the axis in pipe flow, or the vicinity of the external flow in the boundary layer. In 1932, L. Prandtl came to the law (1) using a different approach, but effectively with the same basic assumption. The law (1) is known as the von Kármán–Prandtl universal logarithmic law. More recent derivations which, however, follow the same ideas and the same basic assumption, often in an implicit form, can be found in monographs by Landau & Lifshits (1987), Monin & Yaglom (1971), Schlichting (1968) and in a recent textbook by Spurk (1997).

According to the von Kármán–Prandtl law (1), all experimental points corresponding to the intermediate region should collapse on a single universal straight line in the traditional coordinates $\ln \eta, \phi$.

Subsequent investigations showed, however, that this is not what happens. First, the experiments showed systematic deviations from the universal logarithmic law (1) even if one is willing to tolerate a variation in the constants κ and C (from less than 0.4 to 0.45 for κ, and from less than 5.0 to 6.3 for C). Furthermore, using analytic and experimental arguments, the present authors showed (Barenblatt 1991, 1993; Barenblatt & Prostokishin 1993; Barenblatt, Chorin & Prostokishin 1997*b*; Chorin 1998) that the fundamental von Kármán hypothesis on which the derivation of the universal law (1) was based, i.e. the assumption that the influence of viscosity disappears totally outside the viscous sublayer, is inadequate. In fact, this hypothesis should be replaced by the more complicated one of incomplete similarity, so that the influence of viscosity in the intermediate region remains, but the viscosity enters only in power combination with other factors. This means that the influence of the Reynolds number, i.e. both of the viscosity and the external length scale, e.g. the pipe diameter, remains and should be taken into account in the intermediate region.

For the readers' convenience we present here briefly the concept of incomplete similarity; a more detailed exposition can be found in Barenblatt (1996). The mean velocity gradient $\partial_y u$ in turbulent shear flows can be represented in the general form suggested by dimensional analysis

$$\partial_y u = \frac{u_*}{y} \Phi(\eta, Re).$$

In the intermediate region, $\eta = u_* y/\nu$ is large, and we consider the case of large Reynolds number. The basic von Kármán hypothesis corresponds to the assumption that the dimensionless function $\Phi(\eta, Re)$ at large η and Re can be replaced by a constant $1/\kappa$, its limit as $\eta \to \infty, Re \to \infty$. This corresponds to *complete similarity* both in η and Re. The assumption of *incomplete similarity* in η means that at large η a finite limit of the function Φ does not exist, but that this function can be represented as

$$\Phi = C(Re)\eta^{\alpha(Re)},$$

i.e. the velocity gradient has a *scaling* intermediate asymptotics. Here the functions $C(Re)$ and $\alpha(Re)$ should be specified.

Using some additional analytic and experimental arguments the present authors came to the Reynolds-number-dependent *scaling* law of the form

$$\phi = \frac{u}{u_*} = (C_0 \ln Re + C_1)\eta^{c/\ln Re}, \tag{2}$$

where the constants C_0, C_1 and α must be universal. The scaling law (2) was compared with what seemed (and still seems to us up to now) to be the best available data for turbulent pipe flows, obtained by Nikuradze (1932), under the guidance of Prandtl at his Institute in Göttingen. The comparison has yielded the following values for the coefficients:

$$c = \tfrac{3}{2}, \quad C_0 = \frac{1}{\sqrt{3}}, \quad C_1 = \tfrac{5}{2} \tag{3}$$

when the Reynolds number Re was taken in the form

$$Re = \frac{\bar{u}d}{\nu}. \tag{4}$$

Here $\bar{u}$ is the average velocity (the total flux divided by the pipe cross-section area) and d is the pipe diameter. The final result has the form

$$\phi = \left(\frac{1}{\sqrt{3}}\ln Re + \tfrac{5}{2}\right)\eta^{3/2\ln Re} \tag{5}$$

or, equivalently

$$\phi = \left(\frac{\sqrt{3}+5\alpha}{2\alpha}\right)\eta^{\alpha}, \quad \alpha = \frac{3}{2\ln Re}. \tag{6}$$

The scaling law (5) produces separate curves $\phi(\ln\eta, Re)$ in the traditional $(\ln\eta, \phi)$-plane, one for each value of the Reynolds number. This is the principal difference between the law (5) and the universal logarithmic law (1). We showed that the family (5) of curves having Re as parameter has an envelope, and that in the $(\ln\eta, \phi)$-plane this envelope is close to a straight line, analogous to (1) with the values $\kappa = 0.4$ and $C = 5.1$. Therefore, if the experimental points are close to the envelope they can lead to the illusion that they confirm the universal logarithmic law (1).

The Reynolds-number-dependent scaling law can be reduced to a self-similar universal form

$$\psi = \frac{1}{\alpha}\ln\left(\frac{2\alpha\phi}{\sqrt{3}+5\alpha}\right) = \ln\eta, \quad \alpha = \frac{3}{2\ln Re}, \tag{7}$$

so that contrary to what happens in the $(\ln\eta, \phi)$-plane, in the $(\ln\eta, \psi)$-plane the experimental points should collapse onto a single straight line – the bisectrix of the first quadrant. This statement received a ringing confirmation from the processing of Nikuradze's (1932) data (Barenblatt & Prostokishin 1993; Barenblatt *et al.* 1997*b*).

An important remark should be made here. Izakson, Millikan & von Mises (IMM, see e.g. Monin & Yaglom 1971) gave an elegant derivation of the universal logarithmic law based on what is now known as matched asymptotic expansions. This derivation, which seemed to be unbreakable, persuaded fluid dynamicists that this law was a truth which will enter future turbulence theory essentially unchanged. In the papers of the present authors (Barenblatt & Chorin 1996, 1997), it was demonstrated that the scaling law (2) is compatible with the properly modified IMM procedure. The method of vanishing viscosity (Chorin 1988, 1994) was used in this modification.

Let us turn now to shear flows other than flows in pipes. By the same logic, the scaling law (5) should also be valid for an intermediate region adjacent to the viscous sublayer for all good quality experiments performed in turbulent shear flows at large Re.

The first question is, what is the appropriate definition of the Reynolds number for these flows which will make the formula (5) applicable? This is a very important point – if the universal Reynolds-number-independent logarithmic law were valid, the definition of the Reynolds number would be irrelevant provided it were sufficiently large. For the scaling law (5) this is not the case. Indeed, if the scaling law (5) has general applicability it should be possible to find, for every turbulent shear flow at large Reynolds number, an appropriate definition of the Reynolds number which will make the scaling law (5) valid.

There exists nowadays a large amount of data for an important class of wall-bounded turbulent shear flows: turbulent zero-pressure-gradient boundary layers. These data were obtained over the last 25 years by various authors using various set-ups. For boundary layers the traditional definition of the Reynolds number is

$$Re_\theta = \frac{U\theta}{\nu} \tag{8}$$

where U is the free-stream velocity, and θ is a characteristic length scale – the momentum displacement thickness. The question which we asked ourselves was, is it possible to find for each of these flows a particular lengthscale Λ, so that the scaling law (5) will be valid for all of them with the same values of the constants. Of course, in each case the length scale Λ could be influenced by the contingencies of the particular experiment, but the question of decisive importance is whether such a length scale exists. The answer within the accuracy of the experiments is affirmative.

We present here the results of the processing all the experimental data available to us, in particular all the data collected in a very instructive review by Fernholz & Finley (1996). We show that for all of these flows, without any exception, the scaling law (5) is observed with an appropriate accuracy over the whole intermediate region, if the Reynolds number is defined properly, i.e. if the characteristic length Λ entering the Reynolds number

$$Re = \frac{U\Lambda}{\nu} \tag{9}$$

is properly determined. Moreover, we show that for all the flows where the turbulence in the external flow is small, there exists a sharply distinguishable second intermediate region between the first one where the scaling law (5) is valid and the external homogeneous flow. The average velocity distribution in this second intermediate region is also self-similar of scaling type:

$$\phi = B\eta^\beta \tag{10}$$

where B and β are constants.

However, a Reynolds-number dependence of the power β was not observed. Within the accuracy of the experimental data β is close to $1/5$. When the turbulence in the external homogeneous flow becomes significant, the second self-similar region becomes smaller and the power β decreases with growing external turbulence until the second intermediate region disappears completely.

2. The first group of zero-pressure-gradient boundary layer experiments

We will explain later why we divided the experimental data into three groups. Here it is sufficient to note that all available sets of experimental data were eventually taken into account.

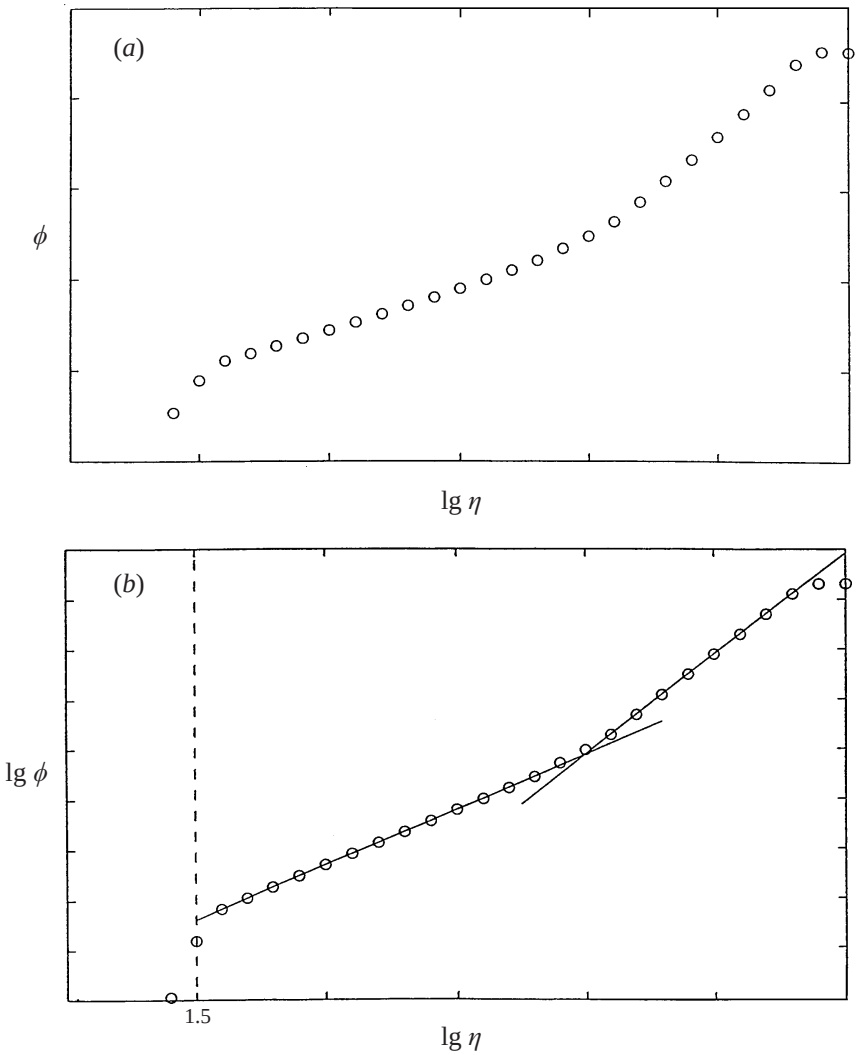

FIGURE 1. (*a*) Schematic representation of the experimental data in traditional coordinates $\ln\eta, \phi$. (*b*) Schematic representation of the experimental data in $(\lg\eta, \lg\phi)$ coordinates for experiments of the first group.

The original data were always presented by their authors in the form of graphs in the traditional $(\ln\eta, \phi)$-plane, suggested by the universal logarithmic law (1). The shape of the original graphs was always similar to the one presented qualitatively in figure 1(*a*). Therefore, the first rather trivial step was to replot the data in the doubly logarithmic coordinates $(\lg\eta, \lg\phi)$ appropriate for revealing the scaling laws. The result was instructive: for all experiments of the first group (in chronological order), specifically: Collins, Coles & Hike (1978)†; Erm & Joubert (1991); Smith (1994)†; Naguib (1992)‡, and Nagib & Hites (1995)‡; Krogstad & Antonia (1999), the data outside the viscous sublayer ($\lg\eta > 1.5$) have the characteristic shape of a broken line, shown qualitatively in figure 1(*b*) and quantitatively in figures 2–6.

† The data were obtained by scanning the graphs in the review by Fernholz & Finley (1996).
‡ The data in digital form were provided to us by Dr M. Hites.

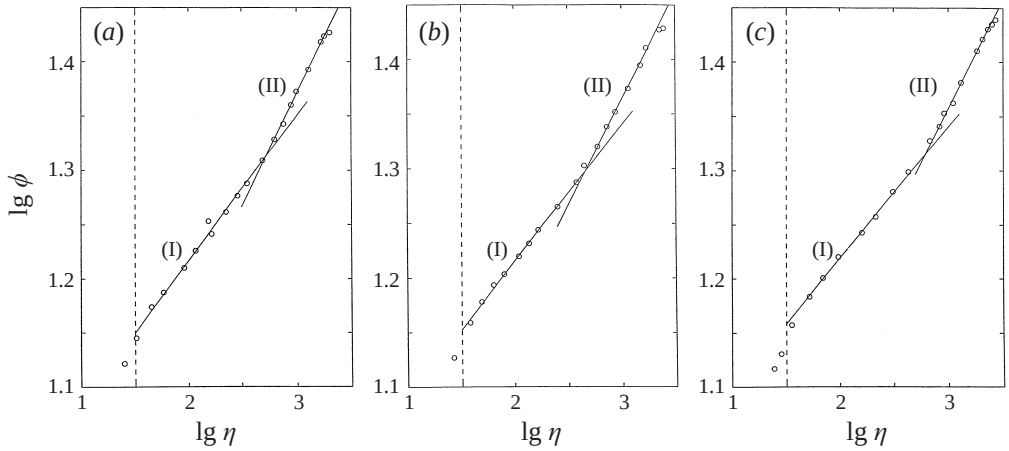

FIGURE 2. The experiments by Collins, Coles & Hike (1978) (data taken from Fernholz & Finley 1996). (*a*) $Re_\theta = 5938$, (*b*) $Re_\theta = 6800$, (*c*) $Re_\theta = 7880$. Both self-similar intermediate regions (I) and (II) are clearly seen.

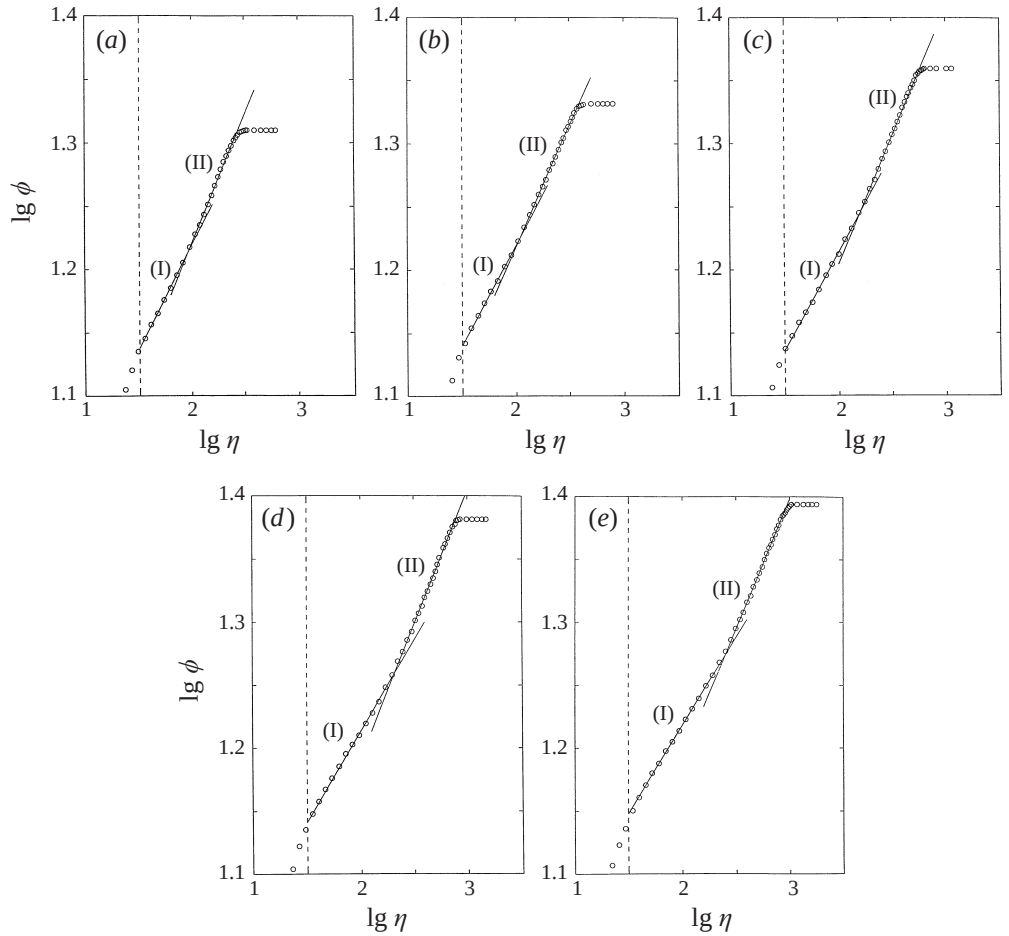

FIGURE 3. The experiments by Erm & Joubert (1991). (*a*) $Re_\theta = 697$, (*b*) $Re_\theta = 1003$, (*c*) $Re_\theta = 1568$, (*d*) $Re_\theta = 2226$, (*e*) $Re_\theta = 2788$. Both self-similar intermediate regions (I) and (II) are clearly seen.

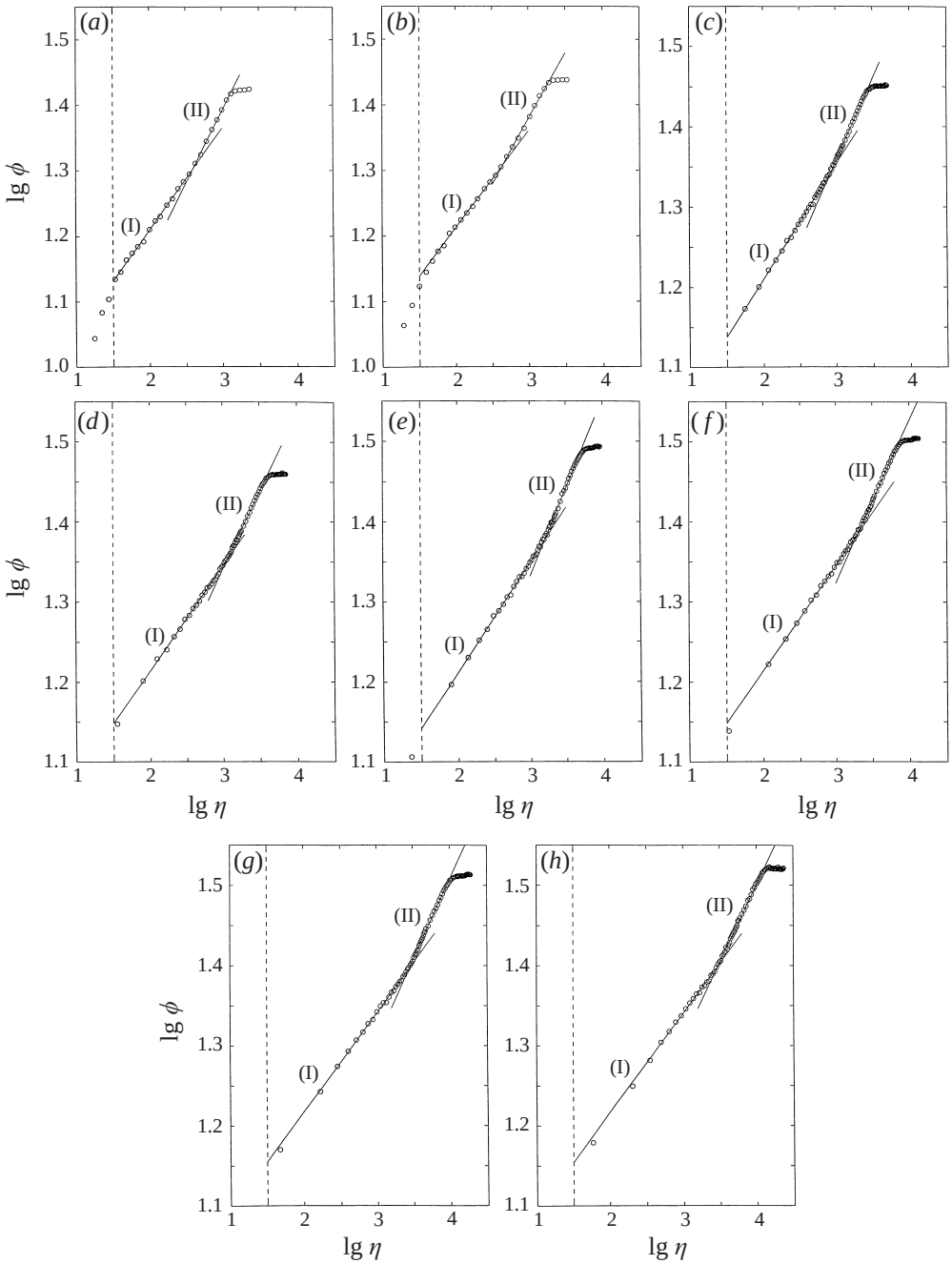

FIGURE 4. (*a,b*) The experiments by Naguib (1992): (*a*) $Re_\theta = 4550$, (*b*) $Re_\theta = 6240$. Both self-similar intermediate regions (I) and (II) are clearly seen. (*c–h*) The experiments by Nagib & Hites (1995): (*c*) $Re_\theta = 9590$, (*d*) $Re_\theta = 13\,800$, (*e*) $Re_\theta = 21\,300$, (*f*) $Re_\theta = 29\,900$, (*g*) $Re_\theta = 41\,800$, (*h*) $Re_\theta = 48\,900$. Both self-similar intermediate regions (I) and (II) are clearly seen.

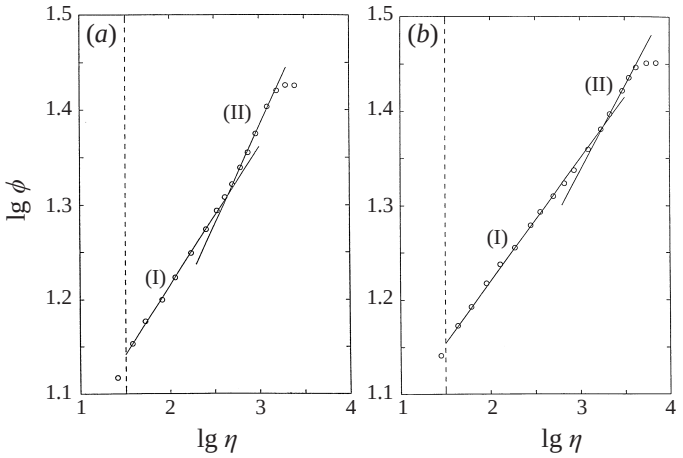

FIGURE 5. The experiments of Smith (1994) (data taken from Fernholz & Finley 1996). (*a*) $Re_\theta = 4996$, (*b*) $Re_\theta = 12\,990$. The first self-similar intermediate region (I) is clearly seen, the second region (II) can be revealed.

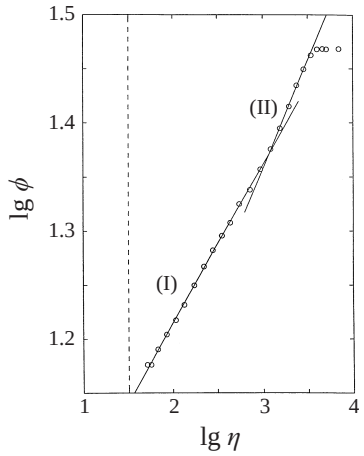

FIGURE 6. The experiments of Krogstad & Antonia (1998). $Re_\theta = 12\,570$. Both self-similar intermediate regions (I) and (II) are clearly seen.

Thus, the two straight lines forming the broken line that were revealed in the $(\lg\eta, \lg\phi)$-plane have as equations

$$\text{(I)} \quad \phi = A\eta^{\alpha}; \quad \text{(II)} \quad \phi = B\eta^{\beta}. \tag{11}$$

The coefficients A, α, B, β were obtained by us through statistical processing.

We assume as before that the effective Reynolds number Re has the form (9): $Re = U\Lambda/\nu$, where U is the free-stream velocity and Λ is a length scale. The basic question is, whether one can find in each case a length scale Λ which plays the same role for the intermediate region (I) of the boundary layer as the diameter does for pipe flow. In other words, whether it is possible to find a length scale Λ, perhaps influenced by individual features of the flow, so that the scaling law (5) is valid for the first intermediate region (I). To answer this question we have taken the values of A and

Figure	Re_θ	α	A	$\ln Re_1$	$\ln Re_2$	$\ln Re$	Re_θ/Re	β
				Collins, Coles & Hiks (1978)				
2(*a*)	5938	0.129	9.10	11.43	11.63	11.53	0.06	0.203
2(*b*)	6800	0.125	9.23	11.66	12.00	11.83	0.05	0.195
2(*c*)	7880	0.123	9.41	11.97	12.21	12.09	0.04	0.202
				Erm & Joubert (1991)				
3(*a*)	697	0.163	7.83	9.23	9.20	9.22	0.07	0.202
3(*b*)	1003	0.159	7.96	9.46	9.43	9.45	0.08	0.192
3(*c*)	1568	0.156	7.97	9.47	9.62	9.54	0.11	0.202
3(*d*)	2226	0.148	8.26	9.98	10.14	10.06	0.10	0.214
3(*e*)	2788	0.140	8.66	10.67	10.71	10.69	0.06	0.206
				Naguib (1992) and Hites & Nagib (1995)				
4(*a*)	4550	0.156	7.87	9.30	9.62	9.46	0.36	0.22
4(*b*)	6240	0.148	8.24	9.94	10.14	10.04	0.27	0.20
4(*c*)	9590	0.143	8.37	10.17	10.49	10.33	0.31	0.206
4(*d*)	13 800	0.131	8.94	11.15	11.45	11.30	0.17	0.193
4(*e*)	21 300	0.138	8.61	10.58	10.87	10.73	0.47	0.22
4(*f*)	29 900	0.130	8.99	11.24	11.54	11.39	0.34	0.204
4(*g*)	41 800	0.124	9.30	11.78	12.10	11.94	0.27	0.201
4(*h*)	48 900	0.124	9.28	11.74	12.10	11.92	0.33	0.192
				Smith (1994)				
5(*a*)	4996	0.146	8.36	10.15	10.27	10.21	0.18	0.20
5(*b*)	12 990	0.129	9.19	11.59	11.63	11.61	0.12	0.167
				Krogstad & Antonia (1999)				
6	12 570	0.146	8.38	10.18	10.27	10.23	0.45	0.201

TABLE 1. Values of parameters for the first group of experiments.

α, obtained by statistical processing of the experimental data in the first intermediate scaling region, and then calculated $\ln Re_1$, $\ln Re_2$, by solving the equations suggested by the scaling law (5):

$$\frac{1}{\sqrt{3}}\ln Re_1 + \tfrac{5}{2} = A, \quad \frac{3}{2\ln Re_2} = \alpha. \tag{12}$$

If these values of $\ln Re_1$, $\ln Re_2$ obtained by solving the two different equations (12) are indeed close, i.e. if they coincide within experimental accuracy, then the unique length scale Λ can be determined and the experimental scaling law in region (I) coincides with the basic scaling law (5).

Table 1 shows that these values are close, the difference slightly exceeds 3% in only two cases; in all other cases it is less. Thus, for instance, we can introduce for all these flows the mean Reynolds number

$$Re = \sqrt{Re_1 Re_2}, \quad \ln Re = \tfrac{1}{2}(\ln Re_1 + \ln Re_2) \tag{13}$$

and consider Re as an estimate of the effective Reynolds number of the boundary layer flow. Naturally, the ratio $Re_\theta/Re = \theta/\Lambda$ is different for different flows.

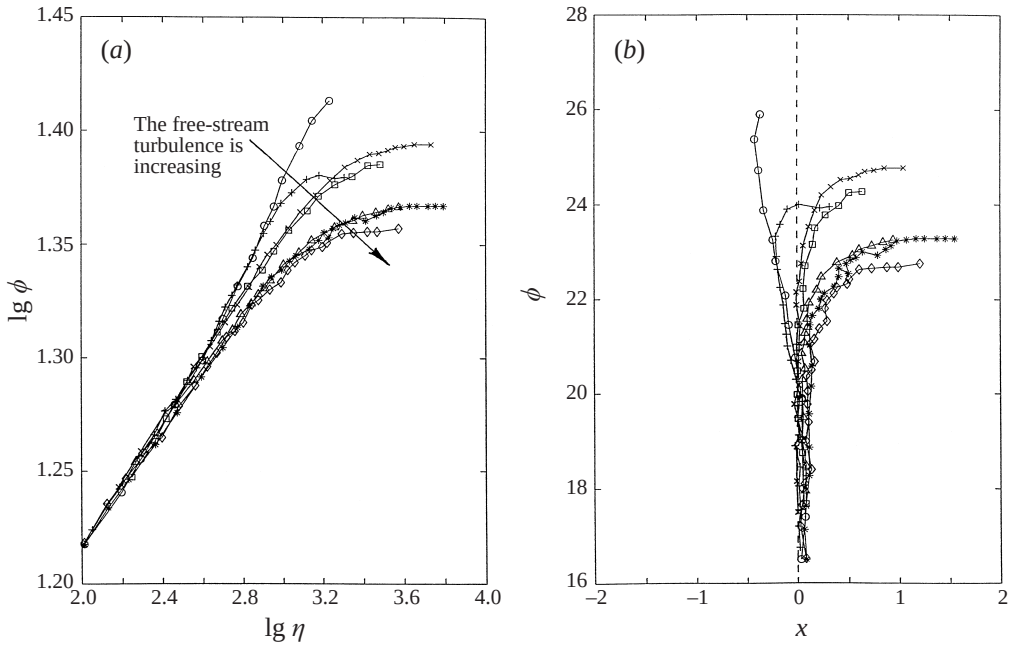

FIGURE 7. (*a*) The experiments by Hancock & Bradshaw (1989) – a general view: ○, see figure 8(*a*); +, see figure 8(*b*); ×, see figure 8(*c*); □, see figure 8(*d*); Δ, see figure 8(*e*); ◇, see figure 8(*f*); ∗, see figure 8(*g*). (*b*) The same data as in (*a*) with the coordinates $(x = \ln\eta - \frac{2}{3}\ln Re(\ln[\phi(\frac{5}{2} + \ln Re/\sqrt{3})]), \phi)$. The deviations from the axis $x = 0$ reflect the influence of the turbulence of the free stream.

Figure	Re_θ	α	A	$\ln Re_1$	$\ln Re_2$	$\ln Re$	u'/U	Re_θ/Re	β
8*a*	4680	0.140	8.66	10.67	10.71	10.69	0.0003	0.11	0.20
8*b*	2980	0.138	8.77	10.86	10.91	10.88	0.024	0.06	0.18
8*c*	5760	0.137	8.80	10.91	10.95	10.93	0.026	0.10	—
8*d*	4320	0.150	8.22	9.91	10.00	9.95	0.041	0.21	—
8*e*	3710	0.122	9.49	12.11	12.30	12.20	0.040	0.02	—
8*f*	3100	0.128	9.13	11.48	11.70	11.59	0.058	0.03	—
8*g*	3860	0.129	9.07	11.38	11.63	11.50	0.058	0.04	

TABLE 2. Parameters for the experiments by Hancock & Bradshaw.

3. Zero-pressure-gradient boundary layer beneath a turbulent free stream: the experiments of Hancock & Bradshaw

The experiments of Hancock & Bradshaw (1989) revealed a new feature important for our analysis. Examination of these experimental data suggested that we separate the other experiments into two groups. In the Hancock & Bradshaw experiments the free stream was made turbulent by a grid in all series, except one. Thus, processing the data from these experiments we were able not only to compare the scaling law (5) with experimental data once again but also to investigate the influence of the turbulence of the external flow on the second self-similar intermediate region. The results of the processing are presented in table 2 and figures 7 and 8. In both table 2

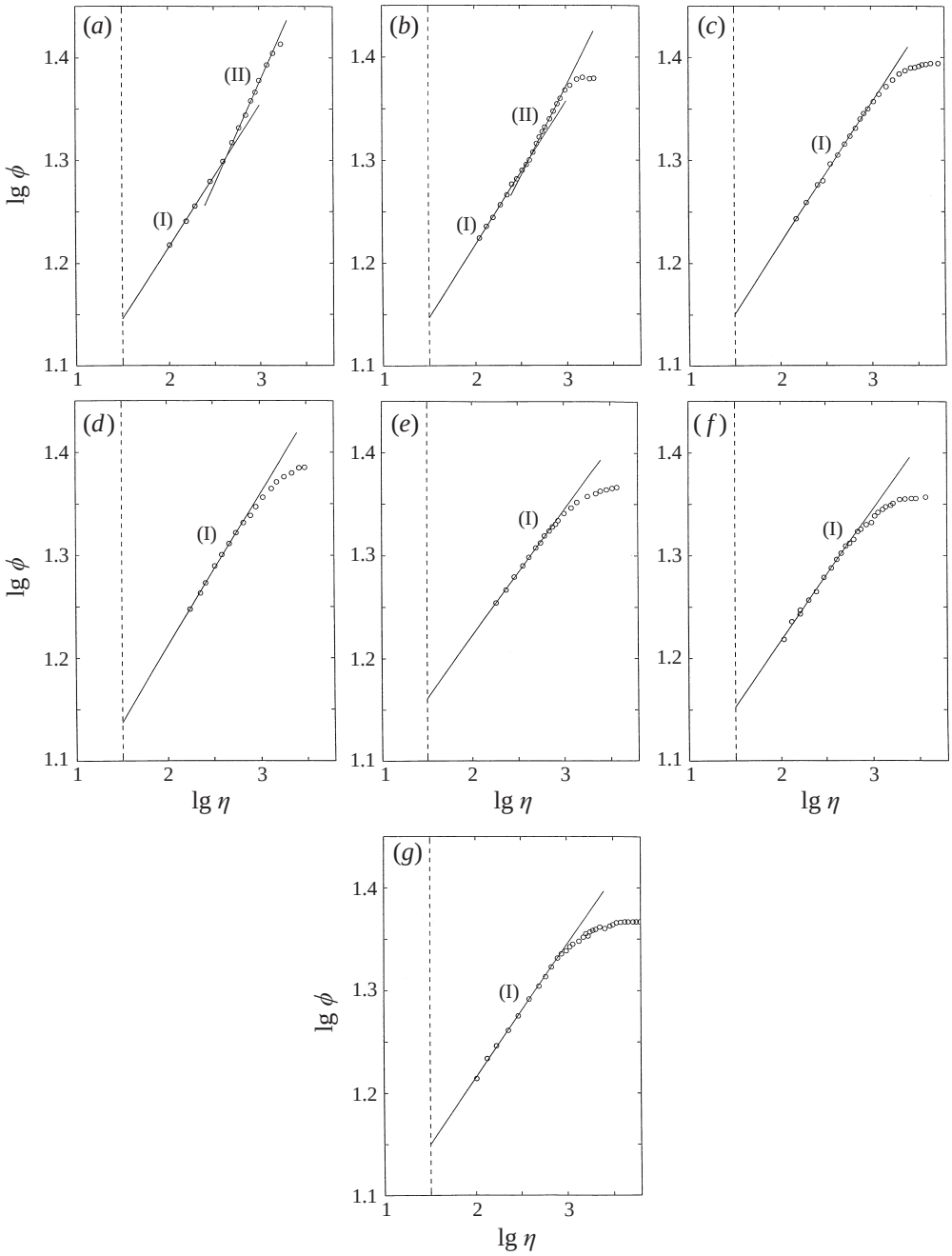

FIGURE 8. The experiments by Hancock & Bradshaw (1989). (*a*) $Re_\theta = 4680$, $u'/U = 0.0003$ – both self-similar intermediate regions are clearly seen. (*b*) $Re_\theta = 2980$, $u'/U = 0.024$ – both self-similar intermediate structures (I) and (II) are clearly seen. (*c*) $Re_\theta = 5760$, $u'/U = 0.026$; (*d*) $Re_\theta = 4320$, $u'/U = 0.041$; (*e*) $Re_\theta = 3710$, $u'/U = 0.040$ – the first self-similar intermediate region (I) is clearly seen, the second is not revealed. (*f*) $Re_\theta = 3100$, $u'/U = 0.058$; (*g*) $Re_\theta = 3860$, $u'/U = 0.058$ – the first self-similar intermediate region (I) is seen, although with a larger scatter, the second is not revealed.

Figure	Re_θ	α	A	$\ln Re_1$	$\ln Re_2$	$\ln Re$	Re_θ/Re
				Winter & Gaudet (1973)			
9(*a*)	32 150	0.133	8.86	11.02	11.32	11.17	0.45
9(*b*)	42 230	0.122	9.37	11.90	12.30	12.10	0.24
9(*c*)	77 010	0.115	10.30	13.51	13.04	13.27	0.13
9(*d*)	96 280	0.107	10.56	13.96	14.02	13.99	0.08
9(*e*)	136 600	0.103	10.83	14.43	14.56	14.50	0.07
9(*f*)	167 600	0.101	11.20	15.07	14.85	14.96	0.05
9(*g*)	210 600	0.100	11.15	14.98	15.00	14.99	0.06
				Purtell, Klebanov & Buckley (1981)			
10(*a*)	1002	0.170	7.39	8.47	8.82	8.64	0.18
10(*b*)	1837	0.164	7.62	9.14	8.87	9.00	0.23
10(*c*)	5122	0.149	8.11	9.72	10.07	9.89	0.26
				Erm (1988)			
11(*a*)	2244	0.153	8.04	9.60	9.80	9.70	0.14
11(*b*)	2777	0.154	8.13	9.75	9.74	9.75	0.16
				Petrie, H. L., Fontaine, A. A., Sommer, S. T. and Brungart, T. A. (1990)			
12	35 530	0.119	9.76	12.57	12.61	12.59	0.12
				Bruns, Dengel & Fernholz (1992) and Fernholz, Krause, Nockemann & Schober (1995)			
13(*a*)	2573	0.151	8.46	10.32	9.93	10.13	0.10
13(*b*)	5023	0.144	8.85	11.00	10.42	10.70	0.11
13(*c*)	7139	0.148	8.49	10.37	10.14	10.25	0.25
13(*d*)	16 080	0.142	8.45	10.31	10.56	10.43	0.47
13(*e*)	20 920	0.37	8.51	10.41	10.95	10.68	0.48
13(*f*)	41 260	0.132	8.63	10.62	11.36	10.98	0.70
13(*g*)	57 720	0.130	8.71	10.76	11.54	11.14	0.84
				Djenidi & Antonia (1993)			
14(*a*)	1033	0.154	8.20	9.87	9.74	9.81	0.06
14(*b*)	1320	0.150	8.37	10.17	10.00	10.08	0.06
				Warnack (1994)			
15(*a*)	2552	0.152	8.29	10.03	9.87	9.95	0.12
15(*b*)	4736	0.149	8.20	9.87	10.07	9.97	0.22

TABLE 3. Parameters for the third group of experiments. Data taken from Fernholz & Finley 1996.

and figures 7 and 8 the intensity of turbulence is shown by the value of u'/U, where u' is the mean-square velocity fluctuation in the free stream.

First of all, our processing showed that the first self-similar intermediate layer is clearly seen in all these experiments, both in the absence of the external turbulence,

and in its presence. The values of $\ln Re_1$ and $\ln Re_2$ are close. This means that the basic scaling law (5) is valid in the intermediate region adjacent to the viscous sublayer. At the same time, the second self-similar region is clearly observed and well-defined only when the external turbulence is weak (figure 8*a* and to a lesser extent, figure 8*b*) so that the external turbulence leads to a drastic reduction of the power β, and even to the reduction of the second self-similar intermediate region so that β becomes indeterminate. We illustrate the influence of the free-stream turbulence additionally by figure 7(*b*). Note, from figures 8(*b*) and 8(*c*) the natural fact that a given level of free-stream turbulence has a bigger effect at larger *Re*.

The experiments of Hancock & Bradshaw are instructive because they suggest at least one possible reason for the destruction of the intermediate self-similar region adjacent to the external flow that is observed in the experiments of the next group.

4. The remaining group of zero-pressure-gradient boundary layer experiments

In this section the results of the processing are presented for all the remaining series of experiments. For all of them we used the data presented in the form of graphs in the review of Fernholz & Finley (1996). The results of the processing are presented in table 3 and in figures 9–15.

All the data reveal the self-similar structure in the first intermediate region adjacent to the viscous sublayer. The scaling laws obtained for this region give values of $\ln Re_1$ and $\ln Re_2$ close to each other, although the difference between $\ln Re_1$ and $\ln Re_2$ is sometimes larger than in the experiments of the first group. The scaling law (5) is confirmed by all these experiments. At the same time, for this group of experiments the second self-similar structure adjacent to the free stream turns out to be less clear-cut, if it is there at all. Therefore, for this group of experiments, we did not present the estimates for the values of β. Nevertheless we note that when it was possible to obtain estimates they always gave a β less than 0.2. Note also that for all these experiments the number of experimental points belonging to the region adjacent to the free stream was less than for the experiments of the first group: this was an additional argument for our reluctance to show here the second self-similar layer. As explained in § 3, we suggest that the turbulence of the external flow in the experiments of this remaining group was more significant.

5. Checking universality

The universal form of the scaling law

$$\psi = \frac{1}{\alpha}\ln\left(\frac{2\alpha\phi}{\sqrt{3}+5\alpha}\right) = \ln\eta \tag{14}$$

gives another way to demonstrate clearly the applicability of the scaling law (5) to the first intermediate region of the flow adjacent to the viscous sublayer. According to relation (14), in the coordinates $(\ln\eta, \psi)$, all experimental points should collapse onto the bisectrix of the first quadrant. In figure 16(*a*) are represented the data of Erm & Joubert (1991), Smith (1994), and Krogstad & Antonia (1999). It is seen that the data collapse on the bisectrix with sufficient accuracy to confirm the scaling law

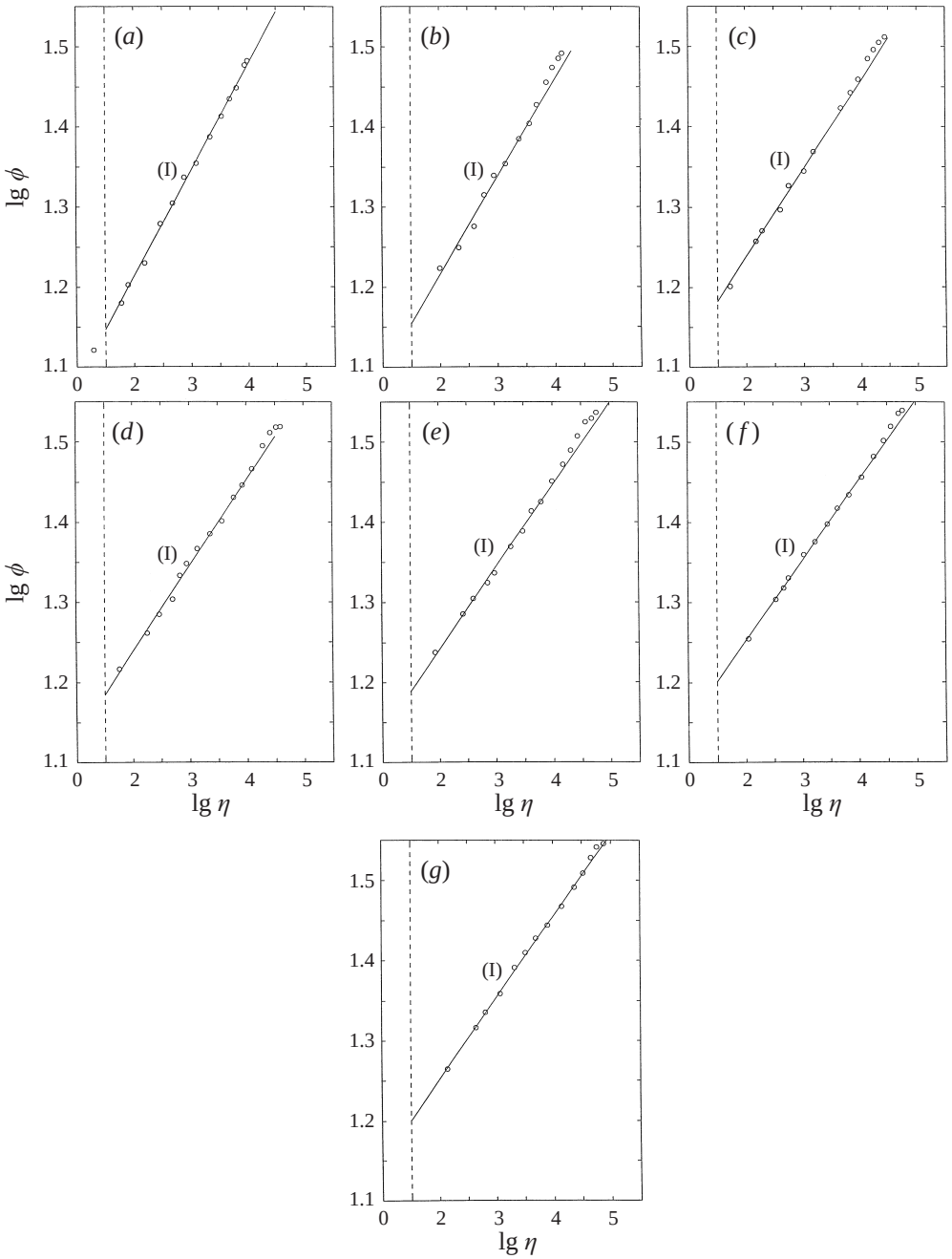

FIGURE 9. The experiments of Winter & Gaudet (1973) (data taken from Fernholz & Finley 1996). (*a*) $Re_\theta = 32\,150$, (*b*) $Re_\theta = 42\,230$, (*c*) $Re_\theta = 77\,010$, (*d*) $Re_\theta = 96\,280$ – the first self-similar intermediate region (I) is seen, although with a larger scatter, the second is not clearly revealed. (*e*) $Re_\theta = 136\,600$ – the first self-similar intermediate region (I) is seen, although with a larger scatter; the number of points is not enough to make a definite estimate for the second region, but the slope β is less than 0.2. (*f*) $Re_\theta = 167\,600$ – the first self-similar intermediate region (I) is seen, although with a larger scatter, the second is not clearly revealed. (*g*) $Re_\theta = 210\,600$ – the first self-similar intermediate region (I) is seen, although with a larger scatter, the second is not revealed.

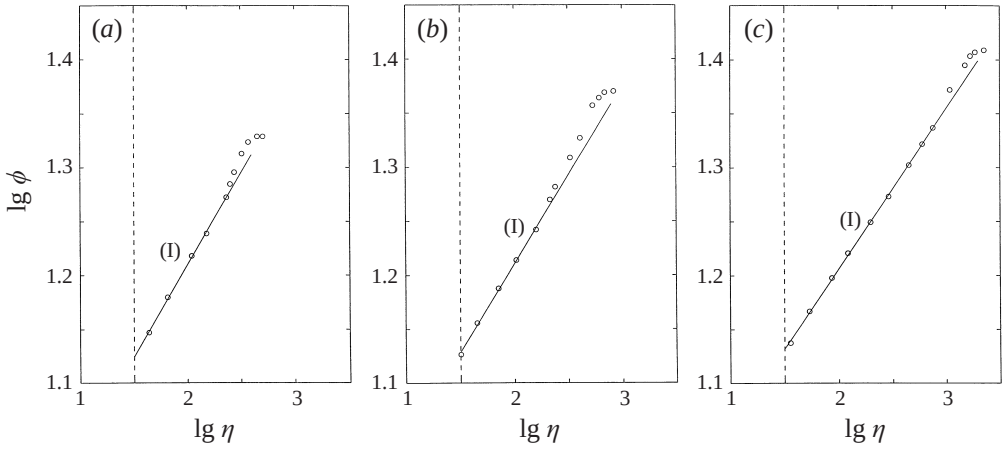

FIGURE 10. The experiments of Purtell, Klebanov & Buckley (1981) (data taken from Fernholz & Finley 1996). (*a*) $Re_\theta = 1002$ – the first self-similar region (I) is revealed in spite of the small number of points, the second self-similar region is not clearly revealed. (*b*) $Re_\theta = 1837$ – the first self-similar region (I) is revealed in spite of the small number of points, the second self-similar region is revealed. (*c*) $Re_\theta = 5122$ – the first self-similar region (I) is revealed, the second self-similar region is not clearly revealed.

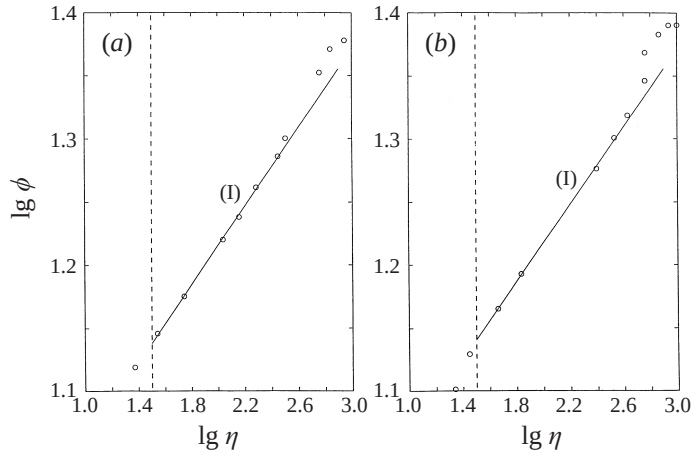

FIGURE 11. The experiments of Erm (1988) (data taken from Fernholz & Finley 1996). (*a*) $Re_\theta = 2244$, (*b*) $Re_\theta = 2777$. The first self-similar region (I) is revealed. The second self-similar region is not revealed.

(5). The parameter α was calculated according to the formula $\alpha = (3/2 \ln Re)$, $\ln Re$ was taken here to be $(\ln Re_1 + \ln Re_2)/2$ (see tables 1 and 3).

In figure 16(*b*) the results of the experiments of Winter & Gaudet (1973), are presented. These experiments are specially interesting because they cover a large range of Reynolds numbers (see table 3). The collapse onto the bisectrix, although with a larger scatter than for the data presented in figure 16(*a*), is clearly demonstrated.

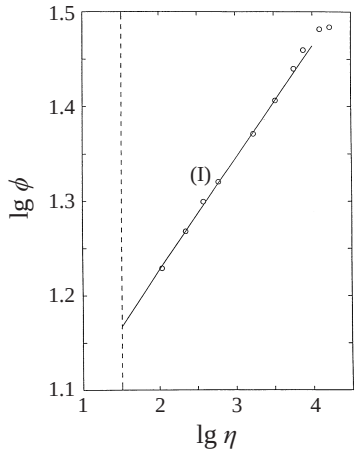

FIGURE 12. The experiments of Petrie, Fontaine, Sommer & Brungart (1990) (data taken from Fernholz & Finley 1996). $Re_\theta = 35\,530$. The first self-similar region (I) is revealed. The second self-similar region is not revealed.

In figure 16(*c*) we present the results of the experiments of Bruns, Dengel & Fernholz (1992), and Fernholz *et al.* (1995). Basically they also collapse onto the bisectrix, although with yet larger scatter, and some systematic deviation at large η. This deviation can be explained, at least partially, by the absence of a sharp outer boundary of the first intermediate region, unlike the situation in the experiments of the first group.

In figure 16(*d*) are presented the results of all the experiments except those by Naguib (1992) and Nagib & Hites (1995), which will be discussed later, and the experiments by Winter & Gaudet and Bruns *et al.* and Fernholz *et al.* which are presented separately in figures 16(*b*) and 16(*c*). As is seen, the correspondence to the universal form (14) of the scaling law (5) is reasonable. By contrast, figure 16(*e*) (i) representing the experiments by Naguib (1992), and Nagib & Hites (1995), shows a systematic deviation, in fact a parallel shift, from the bisectrix of the first quadrant. We have already seen such a shift, in the analysis of the pipe experiments of the Princeton group (Zagarola *et al.* 1996); in our papers on pipe flow (Barenblatt *et al.* 1997*a*, *b*) we concluded that the shift was due to the effects of wall roughness, which increases the effective viscosity. To understand the shift better, we also analysed the data in the paper of Krogstad & Antonia (1998) where a rough wall was used deliberately, albeit for a very large roughness. We did indeed find that in these experiments that the experimental points lie much below the bisectrix. Furthermore, in these experiments $\ln Re_1$ and $\ln Re_2$ differed significantly, and we therefore picked the value of α that corresponds to $\ln Re_1$. The result is a pair of lines parallel to the bisectrix but far below it (figure 16(*e*, ii)).

More generally, it is very likely that any outside cause that increases the level of turbulence should also increase the effective viscosity, and thus shift the points in the $(\ln\eta, \psi)$-plane downwards. A case in point is the set of experiments of Hancock & Bradshaw (1989) discussed above, where turbulence was created by a grid in the free stream. The parallel downward shift is indeed observed (figure 16*f*), and it is of the same order of magnitude as the shift in the experiments of Nagib & Hites. Note that

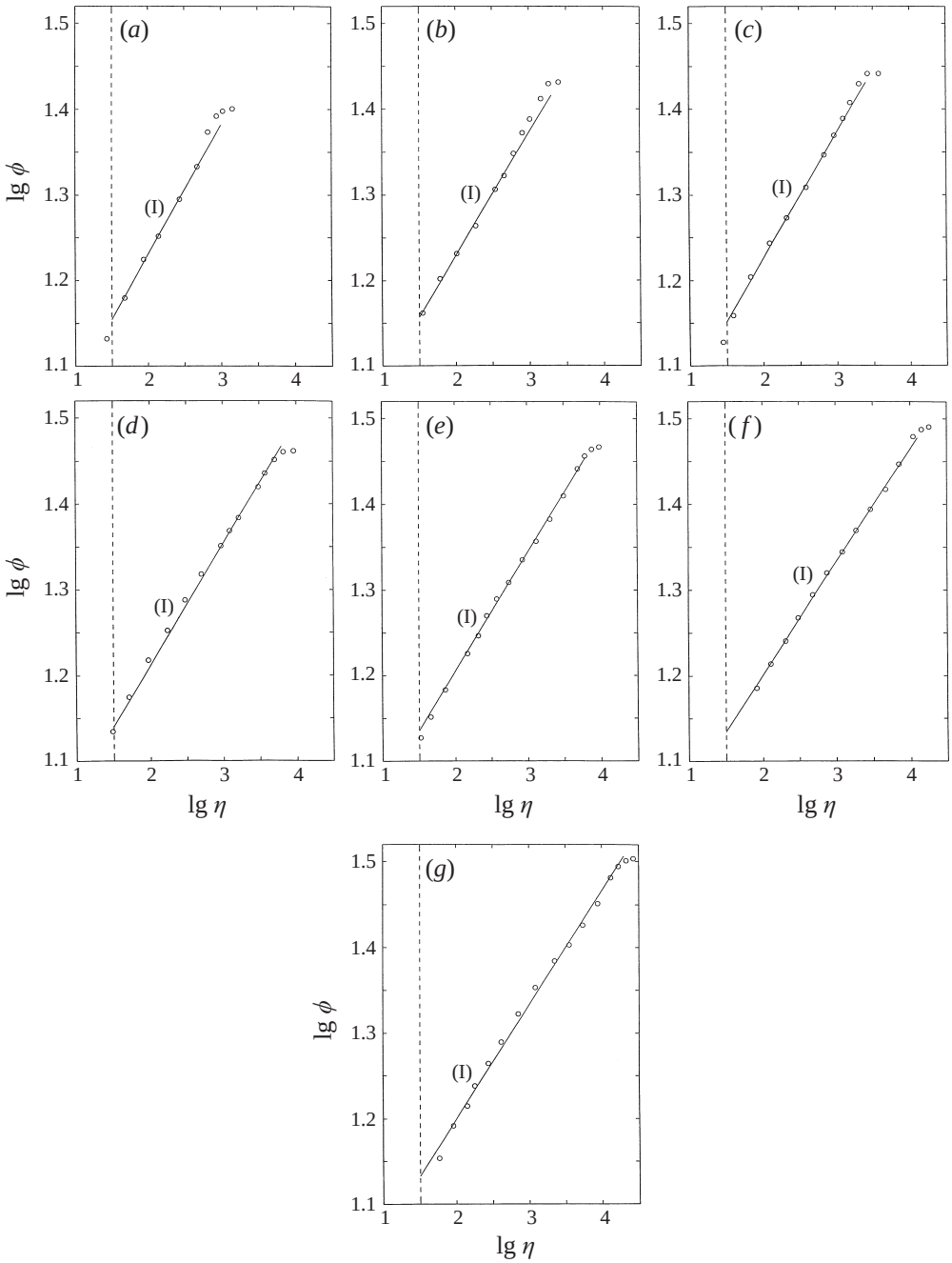

FIGURE 13. The experiments of Bruns, Dengel & Fernholz (1992) and Fernholz, Krause, Nockemann & Schober (1995) (data taken from Fernholz & Finley 1996). (*a*) $Re_\theta = 2573$, (*b*) $Re_\theta = 5023$, (*c*) $Re_\theta = 7139$, (*d*) $Re_\theta = 16\,080$, (*e*) $Re_\theta = 20\,920$, (*f*) $Re_\theta = 41\,260$, (g) $Re_\theta = 57\,720$. The first self-similar region (I) is revealed. The second self-similar region is not revealed.

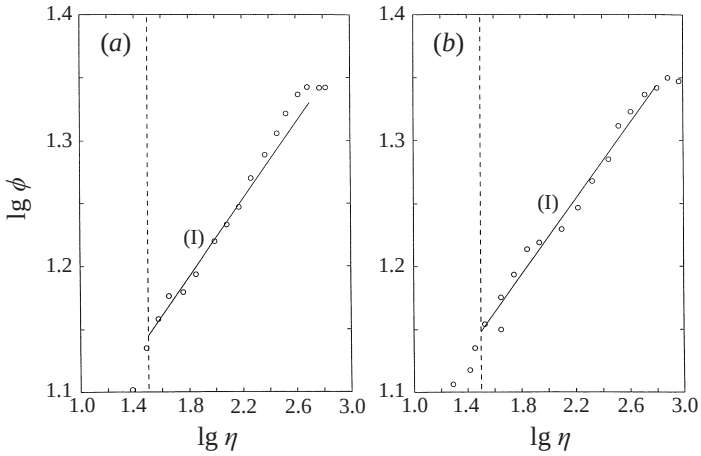

FIGURE 14. The experiments of Djenidi & Antonia (1993) (data taken from Fernholz & Finley 1996). (*a*) $Re_\theta = 1033$ – the first self-similar region (I) is revealed although with a larger scatter, the second self-similar region can be traced. (*b*) $Re_\theta = 1320$ – the first self-similar region (I) is revealed although with a larger scatter, the second self-similar region is not revealed.

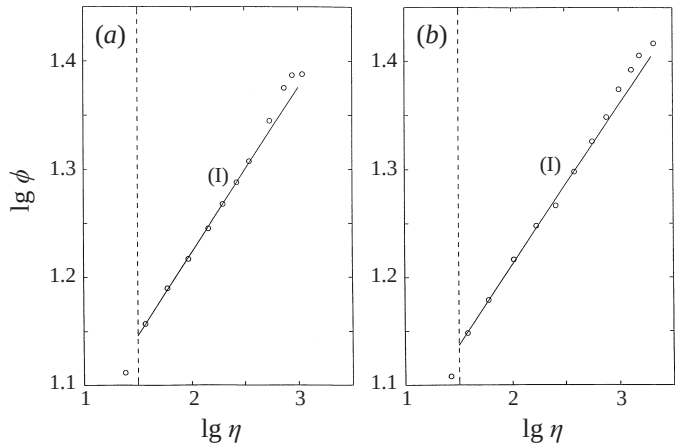

FIGURE 15. The experiments of Warnack (1994) (data taken from Fernholz & Finley 1996). (*a*) $Re_\theta = 2552$, (*b*) $Re_\theta = 4736$. The first self-similar region (I) is clearly seen, the second self-similar region can be traced.

in the experiments of Nagib & Hites the second intermediate region is intact, and it is therefore likely that the shift in the universal description of the first intermediate region is due to the disturbance close to the wall, i.e. to roughness, just as in the experiment of Zagarola *et al.* (1996).

6. Conclusion

The Reynolds-number-dependent scaling law

$$\phi = \frac{u}{u_*} = \left(\frac{1}{\sqrt{3}}\ln Re + \tfrac{5}{2}\right)\eta^{\,3/2\ln Re}, \quad \eta = \frac{u_* y}{\nu} \tag{15}$$

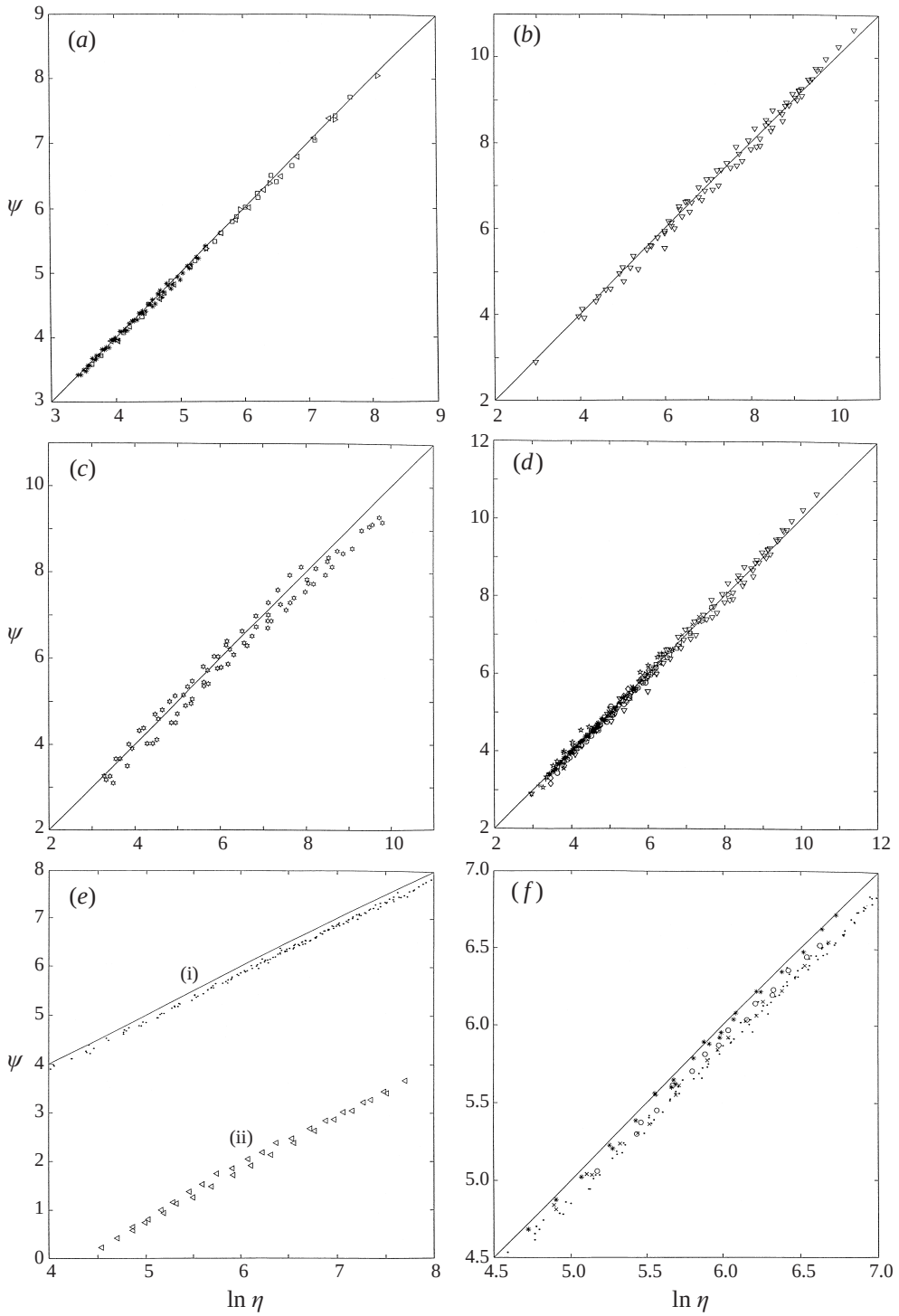

FIGURE 16. For caption see page 282.

was established earlier for the intermediate region of pipe flows between the viscous sublayer and the close vicinity of the pipe axis. The Reynolds number Re was determined as $Re = \bar{u}\,d/\nu$, where $\bar{u}$ is the average velocity, and d the pipe diameter. Attempts (Zagarola & Smits 1998) to adjust the constants of the universal logarithmic law so that this law is valid in a small region near the wall (y less than 0.07 of the pipe radius) are immaterial because these data correspond to the envelope of the family of scaling laws.

In the present work we show that the scaling law (5) gives an accurate description of the mean velocity distribution over the self-similar intermediate region adjacent to the viscous sublayer for a wide variety of zero-pressure-gradient boundary layer flows. The Reynolds number is defined as $Re = U\Lambda/\nu$, where U is the free-stream velocity and Λ is a length scale which is well defined for all the flows under investigation.

We also show that under conditions of weak free-stream turbulence there exists a second intermediate self-similar region between the first one, where the scaling law is valid, and the free stream. This second region becomes smaller under the influence of free stream turbulence.

The validity of the scaling law for boundary layer flows constitutes a strong argument in favour of its validity for a wide class of wall-bounded turbulent shear flows at large Reynolds numbers. The plotting of the experimental data in universal coordinates yields a sensitive gauge of the presence of wall roughness.

Finally, we feel that the affirmation of the effectiveness of incomplete similarity and of vanishing-viscosity asymptotics for turbulent shear flows at large Reynolds numbers has broad implications for other manifestations of turbulence, e.g. in jets, wakes, mixing layers, and local structure, and should lead to a reconsideration of the basic tools used in the study of turbulent flows.

The authors would like to thank Professors P. Bradshaw and P.-A. Krogstad for providing them with their recent data.

This work was supported in part by the Applied Mathematics subprogram of the U.S. Department of Energy under contract DE-AC03-76-SF00098, and in part by the National Science Foundation under grants DMS94-14631 and DMS97-32710.

FIGURE 16. (*a*) The experiments of: ✻, Erm & Joubert (1991); □, Smith (1994); ◁, Krogstad & Antonia (1998); and ▷, Petrie *et al.* (1990). (*b*) ∇, The data of Winter & Gaudet (1973). (*c*) ✻, The data of Bruns *et al.* (1973) and Fernholz *et al.* (1995). (*d*) The data of all experiments except of those by Naguib (1992) and Nagib & Hites (1995), Bruns *et al.* (1992) and Fernholz *et al.* (1995): ○, Collins *et al.* (1978); ▷, Petrie *et al.* (1990); +, Erm (1988); ◇, Putell *et al.* (1981); ✻, Djenidi & Antonia (1993); ×, Warnack (1994); ◁, Krogstad & Antonia (1998); ∇, Winter & Gaudet (1973). All the data in (*a–d*) collapse on the bisectrix of the first quadrant in accordance with the universal form (14) of the scaling law (5). (*e*) (i) The data of Naguib (1992) and Nagib & Hites (1995) show a systematic deviation from the bisectrix of the first quadrant. (ii) The data of Krogstad & Antonia (1998) related to rough walls: the experimental points lie much lower than bisectric. For the evaluation of ψ the value $\alpha = 3/2 \ln Re_1$ was taken. (*f*) The data of Hancock & Bradshaw (1989) show the parallel shift from the bisectrix of the same order as in the experiments by Nagib & Hites: ●, Nagib & Hites; ✻, Hancock & Bradshaw, $u'/U = 0.0003, 0.024, 0.026$; ×, Hancock & Bradshaw, $u'/U = 0.040, 0.041$; ○, Hancock & Bradshaw, $u'/U = 0.058$.

REFERENCES

Barenblatt, G. I. 1991 On the scaling laws (incomplete self-similarity with respect to Reynolds number) in the developed turbulent flow in pipes. *C.R. Acad. Sci. Paris* II, **313**, 309–312.

Barenblatt, G. I. 1993 Scaling laws for fully developed shear flows. Part 1. Basic hypotheses and analysis. *J. Fluid Mech.* **248**, 513–520.

Barenblatt, G. I. 1996 *Scaling, Self-Similarity and Intermediate Asymptotics*. Cambridge University Press.

Barenblatt, G. I. & Chorin, A. J. 1996 Small viscosity asymptotics for the inertial range of local structure and for the wall region of wall-bounded turbulence. *Proc. Natl Acad. Sci. USA* **93**, 6749–6752.

Barenblatt, G. I. & Chorin, A. J. 1997 Scaling laws and vanishing viscosity limits for wall-bounded shear flows and for local structure in developed turbulence. *Commun. Pure Appl. Maths* **50**, 381–398.

Barenblatt, G. I., Chorin, A. J., Hald, O. H. & Prostokishin, V. M. 1997 Structure of the zero-pressure-gradient turbulent boundary layer, 1997. *Proc. Natl Acad. Sci. USA* **94**, 7817–7819.

Barenblatt, G. I., Chorin, A. J. & Prostokishin, V. M. 1997*a* Scaling laws in fully developed turbulent pipe flow: discussion of experimental data. *Proc. Natl Acad. Sci. USA* **94a**, 773–776.

Barenblatt, G. I., Chorin, A. J. & Prostokishin, V. M. 1997*b* Scaling laws in fully developed turbulent pipe flow. *Appl. Mech. Rev.* **50**, 413–429.

Barenblatt, G. I. & Prostokishin, V. M. 1993 Scaling laws for fully developed shear flows. Part 2. Processing of experimental data. *J. Fluid Mech.* **248**, 521–529.

Chorin, A. J. 1988 Scaling laws in the vortex lattice model of turbulence. *Commun. Math. Phys.* **114**, 167–176.

Chorin, A. J. 1994 *Vorticity and Turbulence*. Springer.

Chorin, A. J. 1998 New perspectives in turbulence. *Q. Appl. Maths* **56**, 767–785.

Erm, L. P. & Joubert, P. N. 1991 Low Reynolds-number turbulent boundary layers. *J. Fluid Mech.* **230**, 1–44.

Fernholz, H. H. & Finley, P. J. 1996 The incompressible zero-pressure-gradient turbulent boundary layer: an assessment of the data. *Prog. Aerospace Sci.* **32**, 245–311.

Hancock, P. E. & Bradshaw, P. 1989 Turbulence structure of a boundary layer beneath a turbulent free stream *J. Fluid Mech.* **205**, 45–76.

Kármán, Th. von 1930 Mechanische Ähnlichkeit und Turbulenz. *Proc. 3rd Intl Congress for Applied Mechanics* (ed. C. W. Oseen & W. Weibull), vol. 1, pp. 85–93. AB Sveriges Litografiska Tryckenier, Stockholm.

Krogstad, P.-Å. & Antonia, R. A. 1999 Surface roughness effects in turbulent boundary layers. *Exps. Fluids* **27** 450–460.

Landau, L. D. & Lifshits, E. M. 1987 *Fluid Mechanics*. Pergamon.

Monin, A. S. & Yaglom, A. M. 1971 *Statistical Fluid Mechanics*, vol. 1. MIT Press.

Nagib, H. & Hites, M. 1995 High Reynolds number boundary layer measurements in the NDF. *AIAA Paper* 95-0786.

Naguib, A. N. 1992 Inner- and Outer-layer effects on the dynamics of a turbulent boundary layer. PhD thesis, Illinois Institute of Technology.

Nikuradze, J. 1932 Gesetzmaessigkeiten der turbulenten Stroemung in glatten Rohren. *VDI Forschungheft*, No. 356.

Prandtl, L. 1932 Zur turbulenten Stroemung in Rohren und laengs Platten. *Ergeb. Aerodyn. Versuch.*, Series 4, Goettingen, 18–29.

Schlichting, H. 1968 *Boundary Layer Theory*. McGraw-Hill.

Spurk, J. 1997 *Fluid Mechanics*. Springer.

Zagarola, M. V., Smits, A. J., Orszag, S. A. & Yakhot, V. 1996 Experiments in high Reynolds number turbulent pipe flow. *AIAA Paper* 96-0654.

Zagarola, M. V. & Smith, A. J. 1998 Mean-flow scaling of turbulent pipe flow. *J. Fluid Mech.* **373**, 33–79.